

Short Communication

Effect of Process Parameters for Oxygen Plasma Activation of Carbon Nanofibers on the Characteristics of Deposited Platinum Nanoparticles as Electrocatalyst in Proton Exchange Membrane Fuel Cells

Ulrich Rost^{1,2}, Roxana Muntean^{1,2,}, Gabriela Mărginean¹, César Merino³, Roberto Díez³, Nicolae Vaszilcsin², Michael Brodmann¹*

¹ Westphalian Energy Institute, Westphalian University of Applied Sciences, 45897, Gelsenkirchen, Germany

² Faculty of Industrial Chemistry and Environmental Engineering, Politehnica University Timișoara, 300006 Piața Victoriei 2, Timișoara, Romania

³ Grupo Antolin Ingeniería, SA, Ctra. Madrid - Irún, E09007 Burgos, Spain

*E-mail : roxana.muntean@upt.ro

Received: 22 July 2016 / Accepted: 29 August 2016 / Published: 10 October 2016

In the polymer electrolyte membrane fuel cells (PEMFC) state of the art, rare and expensive platinum group metals (PGM) or PGM alloys are used as catalyst material. Reduction of PGMs in PEMFC electrodes is strongly required to reach cost targets for this technology. An optimal catalyst utilization is achieved in case of nano-structured particles supported on carbon material with a large specific surface area. In this study, graphitic material, in form of carbon nanofibers (CNF), is decorated with Pt particles, serving as catalyst material for PEMFC electrodes with low Pt loading. As a novelty, the effect of oxygen plasma treatment of CNFs previously to platinum particle deposition has been studied. Electrodes are investigated in respect of the optimal morphology, microstructure as well as electrochemical properties. Therefore, samples are characterized by means of scanning electron microscopy combined with energy dispersive X-ray analysis, transmission electron microscopy, thermogravimetry, X-ray diffraction as well as X-ray fluorescence analysis. In order to determine the electrochemical active surface area of catalyst particles, cyclic voltammetry has been performed in 0.5 M sulphuric acid. Selected samples have been investigated in a PEMFC test bench according to their polarization behavior.

Keywords: PEM fuel cell electrocatalysts, Carbon nanofibers, Oxygen plasma activation, Pulsed electroplating.

1. INTRODUCTION

Regarding the transformation of the energy sector into renewable sources based economy, novel storage systems are required in the near future in order to ensure energy supply. Certainly, prospective solutions need to be carbon dioxide emissions free. In this sense, water electrolysis is a potential way for obtaining large amounts of energy in form of hydrogen. Environmental friendly produced hydrogen can be reused for electricity generation in stationary or mobile fuel cell applications. However, in order to develop commercially available solutions, technical as well as cost aspects have to be taken into account [1].

The main function of the catalytic layer (CL) in polymer electrolyte membrane fuel cells (PEMFC) is to provide active sites for the electrochemical reactions occurring at the anode -hydrogen oxidation reaction (HOR) and at the cathode - oxygen reduction reaction (ORR) respectively. According to this, catalytic material is needed in order to break the bonds of gas molecules fed to the fuel cell [2]. Noble metals like Pt or platinum group metals (PGM) are known to be feasible catalysts due to their ability to increase the reaction kinetics and their corrosion stability in acid environment. As electrochemical reactions occur on the surface of catalyst particles, a large active surface within the CL is necessary in order to achieve high power density [3]. Therefore, in current state of the art PEMFCs, active surface is increased by the use of carbon supported catalyst nanoparticles, which are structured directly at the interface between electrolyte membrane and porous electrode material. Structure of CL is also porous as gas molecules diffuse to the catalyst particles. However, for electron transfer, catalyst particles need to be electrically connected and furthermore, for proton exchange, catalyst particles need to be in touch with the membrane. This area, which complies with mentioned conditions is known as three phase reaction zone [4-8].

In order to increase power output and to decrease noble metal loading in PEMFCs respectively, research is carried out on advanced CL architectures, which improve catalyst utilization. Catalyst support material that offer itself a high specific surface area, contribute to a large active catalyst surface within the CL. Furthermore, support material needs to be stable to fuel cell operation, as well as electrical conductive for low-loss electron transfer from anode (HOR) and cathode (ORR) to the catalyst particles. Graphitic nanoparticles are favorable as support material for PGM catalysts as these meet the necessary criterions [9, 10].

Typically, Pt on carbon black catalyst is reported for PEMFCs [11-13]. Here, carbon blacks (e.g. Vulcan XC72) with a particle size of about 40 nm and a specific surface area of about $75 \text{ m}^2 \text{ g}^{-1}$ is used as support for Pt with a particle size in the range of 2 up to 5 nm. Furthermore, interest is on more graphitized (and less turbostratic) carbon supports like carbon nanotubes (CNT) [14–16] or carbon nanofibers (CNF) [9, 17]. In addition, graphene sheets have been studied as support material [18, 19]. However, layers consisting only of graphene sheets or graphene flakes may have disadvantageous properties concerning gas flux due to the formation of a roof tile structure [18]. CNTs and CNFs show high specific surface area and are believed to be superior in comparison to turbostratic graphitic structures (like e.g. typically used carbon blacks). As corrosion resistance against oxygen is higher, this makes them suitable, especially for the use at fuel cell cathodes [20].

It was already reported that oxygen plasma treatment on CNFs results in a formation of functional groups on the graphitic surface. This influences the characteristics of treated particles, increasing the surface energy [21-23]. Furthermore, particles deposition is affected due to the plasma activation process [9]. Different plasma parameters (plasma power, gas flow and pressure or exposure time) have to be carefully set in order to achieve formation of oxygen containing functional groups (hydroxylic, carboxylic or carbonylic) on the CNF's surface.

For this experimental work, CNFs with high specific surface area (up to $200 \text{ m}^2 \text{ g}^{-1}$) produced in industrial scale [24, 25] are decorated with platinum particles, serving as catalyst material for PEMFC electrodes with low noble metal loading. Pulse plating technique, which is performed for this work is a suitable method for electrode preparation with low catalyst content [26-28]. The effect of CNF pre-treatment in radio frequency induced oxygen plasma on electrochemical activity of electrodes has been investigated.

2. EXPERIMENTAL

2.1. Preparation of gas diffusion electrodes

In order to prepare gas diffusion electrodes (GDE), CNF dispersions are spray coated on the porous graphitic substrate (gas diffusion layer type Freudenberg H2315 I2C6). To achieve functional group formation on the graphitic surface, CNFs are activated by means of radio frequency induced oxygen plasma (RF plasma reactor type Plasma Finish RFG 300 RF). Plasma treatment has been carried out in an oxygen/argon environment at 60 Pa. Oxygen flow through the reactor chamber, as well as argon flow, has been set to 0.1 N L min^{-1} . Plasma power was varied from 80 to 150 W for an exposure time of 5 to 30 minutes. Plasma parameters (power and duration) have been investigated and optimized in a previous work [29]. Size for samples, which are applied to membrane electrode assemblies (MEA) for investigation in a PEMFC test bench, was $45 \text{ mm} \times 45 \text{ mm}$ (20.25 cm^2). Samples with 1 cm^2 have been used to investigate the properties of the catalytic material.

Subsequently, CNFs are decorated with Pt nanoparticles by pulsed electrodeposition from hexachloroplatinic acid (Galvatron Platinbad from Wieland Edelmetalle) employing a potentiostat/galvanostat type Materials Mates 510. Current density for pulse plating process has been modified from 0.1 A cm^{-2} up to 0.5 A cm^{-2} in order to obtain an optimal particle size and distribution. The electrolyte was heated up to $60 \text{ }^\circ\text{C}$. The pH-value has been adjusted to a value of 2 by adding hydrochloric acid to the electrolyte solution. Pulse length was set to 1 s and pause length at 60 s. This procedure was repeated twelve times for each specimen preparation.

A typically Pt/C electrocatalyst based GDE has been prepared for comparison with Pt/CNF based samples. A Pt/C (50 wt.-% Pt) dispersion was formulated in isopropanol and spray coated on GDL.

2.2. Analysis of morphology and microstructure

In the frame of this experimental work, electrodes are investigated in respect of optimal morphology and microstructure. Therefore, samples were characterized by means of scanning electron microscopy (SEM) combined with energy dispersive X-ray (EDX) spectroscopy (SEM/EDX type Phillips ESEM XL 30, respectively SEM type Hitachi S4500) and transmission electron microscopy (TEM type FEI CM200). X-ray diffraction (XRD) was used to indicate interlayer spacing of investigated carbon support materials in order to determine the graphitization degree (XRD type Philips X'Pert). Results have been compared with highly oriented pyrolytic graphite (HOPG). With respect to the determination of platinum loading of the prepared GDEs by thermogravimetric analysis (TGA), mass changes were detected due to temperature increase using a Netzsch STA 449 F1 Jupiter instrument. For investigated electrodes, pieces of 1 cm² area have been analyzed. Starting from nearly ambient conditions (30 °C), the samples were completely burnt off with a heating rate of 20 °C min⁻¹ up to 1.200 °C. The samples residues are related to non-flammable metallic components. In order to distinguish the platinum catalyst loading from the metallic content of CNFs (transition metal catalysts, e.g. Ni, Co or Fe used for CNF production), X-ray fluorescence analysis (XRF) has been carried out (XRF spectrometer type SPECTRO MIDEX).

2.3. Electrochemical investigation

In order to determine the electrochemical active surface area (ECSA) of prepared GDEs, cyclic voltammetry (CV) has been performed with the aid of a potentiostat type Ivium Technologies Vertex, in 0.5 M sulphuric acid at room temperature. A galvanic cell type Radiometer Analytical CEC/TH was used in a three-electrode configuration with a Pt counter electrode and a saturated calomel reference electrode (SCE). Scan rate was set at 100 mV sec⁻¹ starting from -0.2 V / SCE up to a vertex potential of 0.8 V / SCE. ECSA was calculated after 200 cycles between starting and vertex potential.

Furthermore, corrosion measurements are carried out in order to identify corrosion resistance of the electrodes in acid environment. Measurements were performed in 0.5 M H₂SO₄ starting from a potential of 0.2 V / SCE to 1.2 V vs. SCE with a scan rate of 0.16 mV s⁻¹.

Membrane electrode assemblies (MEA) are manufactured in order to characterize the samples in a fuel cell test environment. Prepared GDEs are used as anodes. As cathode material, standard GDE with high platinum loading (1 mg cm⁻²) was used. To achieve an improved catalyst connection to the membrane, GDEs are coated with Nafion[®] solution (5 wt.-% in alcohol). MEAs have been prepared by hot pressing the electrode on each side of a proton conductive membrane type Dupont Nafion[®] 212.

In order to determine in-situ polarization behavior, MEA samples are tested in a fuel cell test bench with a controlled electrical load type Höcherl & Hackl type ZS1806NV. The utilized test cell based on hydraulic compression has already been described in detail [30, 31]. *U-i* characteristic plots are measured in constant current mode (stepwise). Starting from open circuit voltage (OCV) at 0 A, load current was increased by steps of 1 A up to the vertex current of 15 A (*i* = 0.75 A cm⁻²). Load current was hold for 2 seconds. Average values for current and corresponding cell voltage are recorded digitally (10 values per step).

3. RESULTS AND DISCUSSION

3.1. Graphitization Degree, Morphology and Microstructure

XRD measurements confirmed the high graphitization degree of investigated CNFs ($90.0 \pm 2.8\%$). Graphitization degree of CNF based electrodes is about 18% higher in comparison to the carbon black based electrocatalyst (about 73%). Table 1 shows the calculated graphitization degree's from XRD measurements.

Table 1. Graphitization degree of selected samples calculated from the XRD measurements

Sample	Graphitization degree [%]
HOPG	100
Pt/CNF	90.0 ± 2.8
Pt/C	73.1 ± 1.8

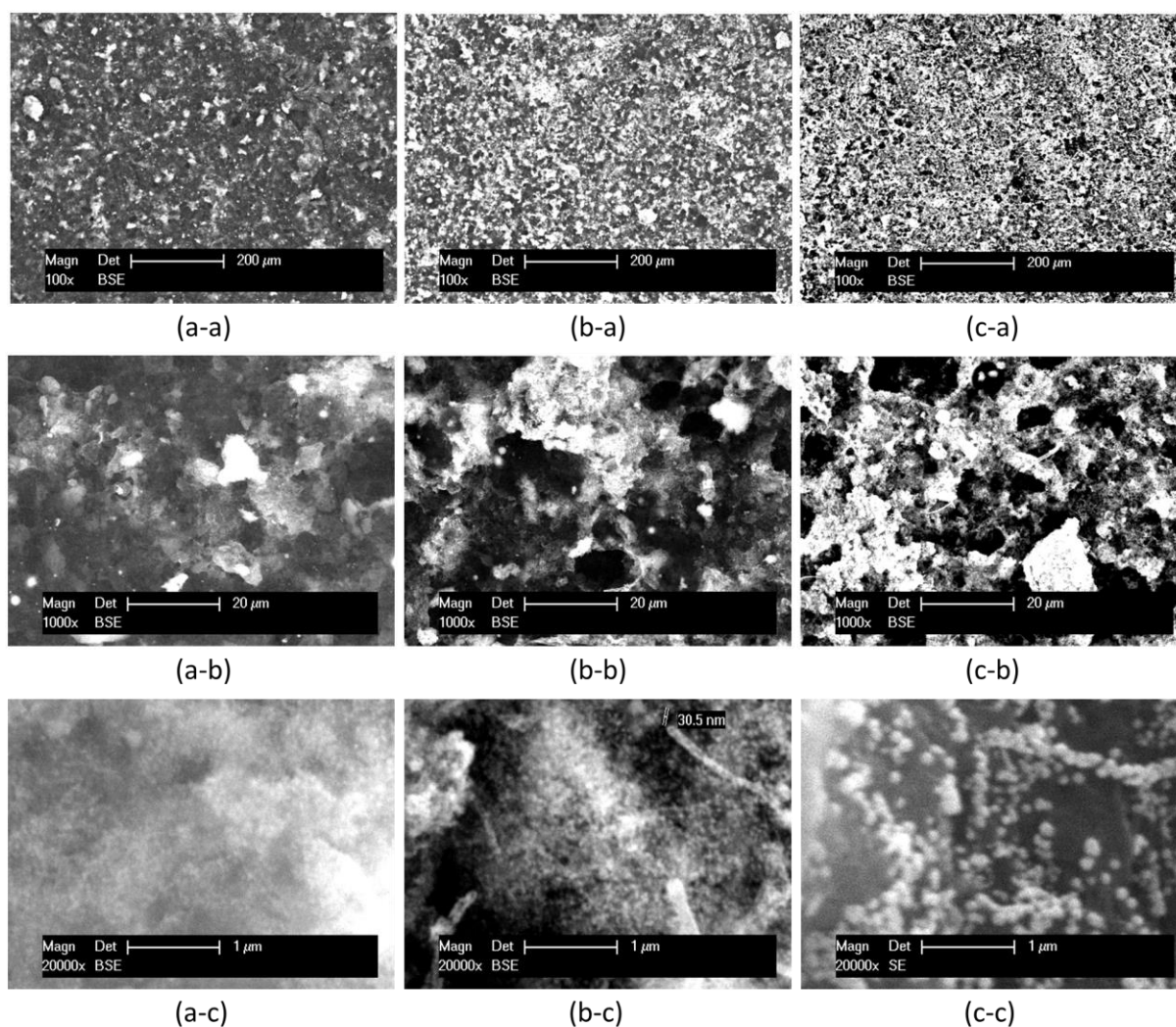


Figure 1. SEM micrographs of Pt/CNF based electrodes depending on current density for Pt particle electrodeposition at different magnifications (a-a; a-b; a-c: $i = 0.1 \text{ A cm}^{-2}$; b-a; b-b; b-c: $i = 0.2 \text{ A cm}^{-2}$; c-a; c-b; c-c: $i = 0.5 \text{ A cm}^{-2}$; SEM- Phillips).

The influence of current density for platinum particle deposition on the morphology and structure of the electrodes has been investigated by SEM (Figure 1). It can be observed that platinum distribution is more homogeneous for particle deposition using higher current density. However, for a deposition current density of 0.5 A cm^{-2} , particle size increases to about 100 nm and clusters start to agglomerate. An optimum platinum particle distribution and cluster size is found when the electrodeposition current density was 0.2 A cm^{-2} . Therefore, Pt/CNF based GDEs further investigated in this work refer to this parameter.

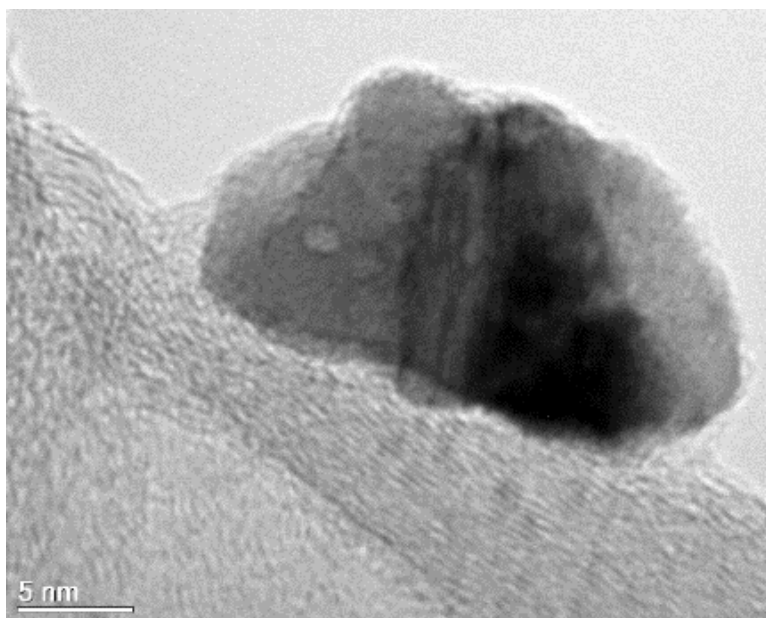


Figure 2. TEM micrograph of a Pt cluster on CNFs obtained using 0.2 A cm^{-2} deposition current density.

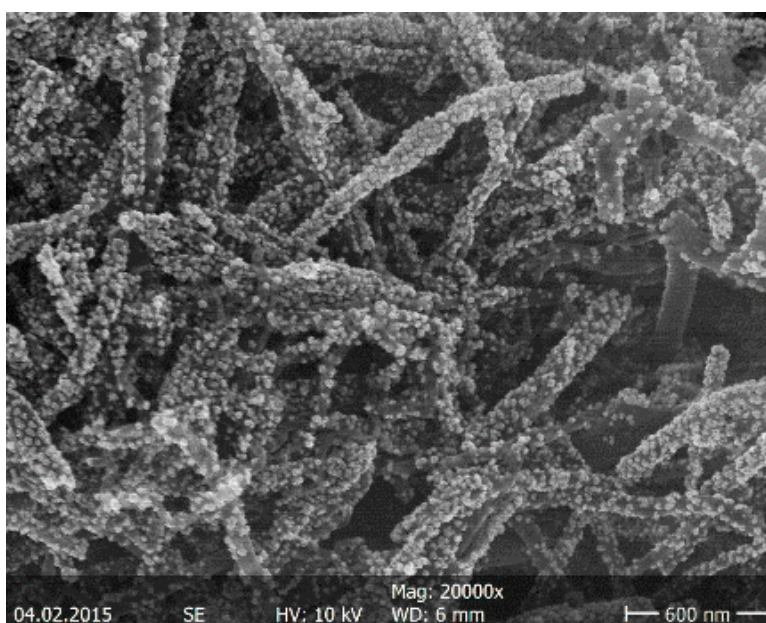


Figure 3. SEM micrograph of Pt particles on CNFs obtained using 0.2 A cm^{-2} deposition current density (SEM - Hitachi).

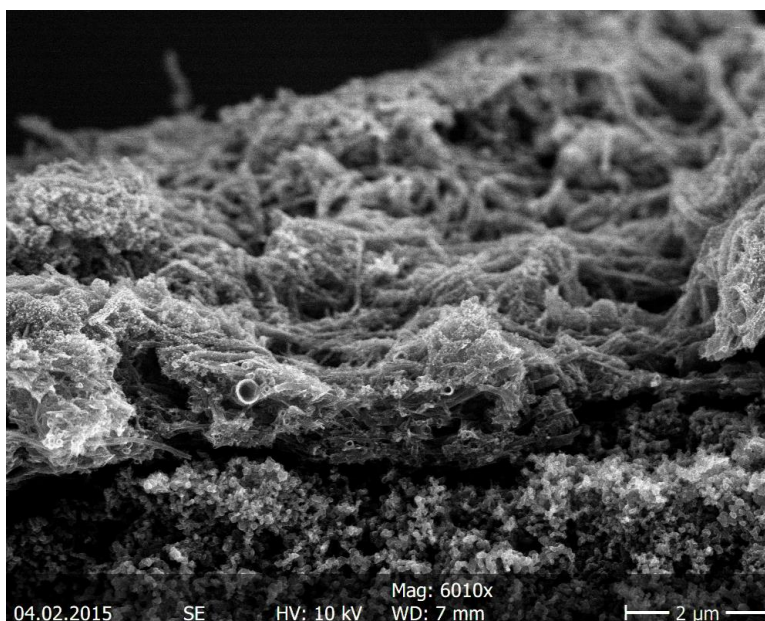


Figure 4. SEM micrograph of Pt particles on CNFs - fracture of a sample (SEM - Hitachi).

TEM, as well as SEM analysis for optimized Pt/CNF based electrodes show clusters of agglomerated Pt particles with the size of about 5 nm. Cluster size is about 30 nm (Fig 2). Furthermore, Pt distribution over the electrode area is nearly homogeneously (Fig. 3). Only less particles have been found within the CNF layer by cross section microscopy and fracture microscopy images (Fig. 4). As a result, localization of Pt particles is favorable for PEMFC electrodes. Concerning particle size and distribution, no influence is observed visually by microscopy due to different plasma treatment.

3.2. Platinum Loading

Table 2. Results from XRF and TG analyses of selected electrode samples depending on CNF loading

Sample	CNF loading [mg cm ⁻²]	Pt content [%]	Residual mass [mg cm ⁻²]	Pt loading [mg cm ⁻²]
GDL substrates blank	-	-	0.030 ± 0.001	-
GDLs with CNFs only	0.5	-	0.096 ± 0.020	-
Pt/CNF	0.15	84.8 ± 0.4	0.160	0.110
Pt/CNF	0.3	85.4 ± 1.5	0.289	0.221
Pt/CNF	0.5	82.3 ± 0.7	0.382	0.290

Platinum loading of prepared electrodes has been determined by TGA. Metallic electrode content is analyzed by XRF in order to distinguish platinum from CNF catalysts, which occur due to the fibers production. XRF measurements are performed at three different points of a sample. CNF

growth catalyst is found to be only nickel. Platinum loading of prepared electrodes depending on CNF loading is given in Table 2.

For blank GDL samples, residues determined by TGA belong to organic content. About 0.03 mg cm^{-2} need to be subtracted for the calculation of platinum loading due to GDL residue. Ni content is determined to be in the range of $13.2\% \pm 4\%$ ($0.132 \pm 0.04 \text{ mg Ni/mg CNF}$). The platinum ratio from metallic content of prepared samples remains nearly constant with varying CNF loading (82.3% to 85.4%). This means that the platinum loading is highly dependent on the CNF loading of a sample.

Furthermore, influence of oxygen plasma treatment is observed. Investigation has been carried out for samples with a CNF loading of about 0.2 mg cm^{-2} .

Table 3 gives information about platinum ratio of metallic content and platinum loading of selected samples depending on the plasma treatment. Electrochemical investigations are carried out with these samples previously to TGA.

Table 3. Results from XRF and TGA analyses of selected samples depending on plasma treatment

Sample	Pt content [%]	Residual mass [mg cm^{-2}]	Pt loading [mg cm^{-2}]
Pt/CNF no plasma	85.3 ± 6.8	0.189 ± 0.025	0.135 ± 0.026
Pt/CNF 80 W 30 min	93.0 ± 0.5	0.172 ± 0.017	0.132 ± 0.018
Pt/CNF 100 W 20 min	94.1 ± 0.4	0.124 ± 0.025	0.088 ± 0.026
Pt/CNF 120 W 10 min	93.9 ± 0.8	0.145 ± 0.011	0.108 ± 0.012
Pt/CNF 150 W 5 min	81.0 ± 0.2	0.136 ± 0.002	0.086 ± 0.003
Pt/C no plasma	100	0.162 ± 0.005	0.132 ± 0.006

Platinum loading of selected electrode samples varies from 0.086 to 0.135 mg cm^{-2} . One can observe that the mass ratio of platinum from metallic electrode content changes with the parameters for plasma treatment. Highest mass fraction is found for plasma activation with 100 W and a treatment time of 20 minutes. Electrodes treated in this circumstances have a platinum mass fraction 10.3% higher than for samples without plasma activation. Samples, which are plasma activated at 150 W, for 5 minutes, show slightly lower platinum loading. However, a mass ratio for platinum is below those for samples without previous plasma treatment. This fact can be explained due to a dominant etching effect of plasma process. Therefore, these samples have not been considered for electrochemical investigation.

3.3. Electrochemical Investigations

CVs for selected samples carried out in $0.5 \text{ M H}_2\text{SO}_4$ are shown in Fig 5. It was found that hydrogen adsorption and hydrogen desorption occurs between -0.2 and 0.1 V vs. SCE. For each plasma parameter, three electrodes are investigated. The peaks A and B, correspond to the atomic H formation and adsorption ($\text{H}_3\text{O}^+ + \text{e}^- \rightarrow \text{H}_{\text{ads}}$), and H_2 formation and adsorption ($\text{H}_{\text{ads}} + \text{H}_3\text{O}^+ + \text{e}^- \rightarrow \text{H}_{2(\text{ads})} + \text{H}_2\text{O}$) respectively. Peak currents for A and B are almost directly proportional to catalytic activity of the electrodes for hydrogen evolution reaction. Similarly, peaks C and D correspond to H_2 and H oxidation. That means the highest catalytic activity is found for the sample treated in oxygen

plasma (120 W for 10 minutes). In addition, an anodic region E, where CNFs are oxidized, is emphasized, as well as region F - just for metallic Pt - in which Pt-oxide is formed. Further, cathodic peak G is assigned to Pt-oxide reduction [32, 33]. Charge associated with the hydrogen desorption is calculated from the area below the plot by numerical integration. ECSA is obtained by dividing the calculated charge with the charge for a polycrystalline platinum surface ($210 \mu\text{C cm}^{-2}$) [33]. CV analysis of prepared GDEs presents the ECSA values, depending on the plasma process. Calculated values of ECSAs, as well as specific ECSAs can be found in Table 4.

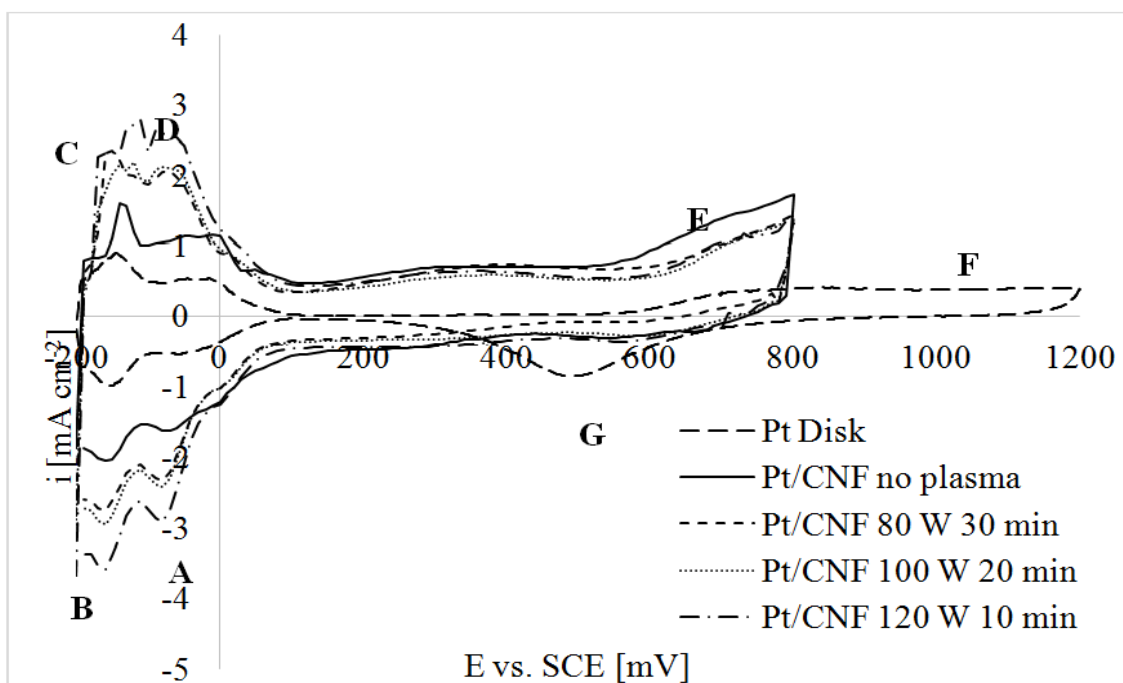


Figure 5. Cyclic voltammograms of selected electrode samples in 0.5 M H_2SO_4 aqueous solution, scan rate 100 mV s^{-1} .

Table 4. ECSA of selected electrode samples depending on plasma treatment calculated from the CV measurements performed in 0.5 M H_2SO_4 aqueous solution

Sample	ECSA [cm^2]	Specific ECSA [$\text{cm}^2 \text{mg}^{-1}$]
Polycrystalline Pt disk	1.01	-
Pt/CNF no plasma	6.44 ± 0.07	47.7
Pt/CNF 80 W 30 min	13.55 ± 0.06	102.7
Pt/CNF 100 W 20 min	11.97 ± 2.31	136.4
Pt/CNF 120 W 10 min	16.03 ± 0.75	148.6

For prepared electrodes, CNF functionalization in RF oxygen plasma at 120 W for 10 minutes provides an increased specific ECSA of $148.6 \text{ cm}^2 \text{mg}^{-1}$, which is 3.1 times higher in comparison to samples without previous plasma activation ($47.7 \text{ cm}^2 \text{mg}^{-1}$). Similar studies have shown that a superior catalytic activity correlated with a high ECSA was obtained for plasma treated carbon nanotubes supported catalysts for electrochemical methanol oxidation [34]. As platinum loading is

slightly higher for electrode samples without activation, higher platinum utilization is achieved when a pre-treatment is applied. This may be explained due to formation of smaller particles, which are distributed more homogeneously on the CL surface as a result of functional groups formation on the fibers surface.

By electrochemical analysis of the corrosion behavior in 0.5 M H₂SO₄, corrosion current is determined for Pt/CNF electrocatalyst according to the optimized preparation route, as well as, for Pt/C based electrodes (Figure 6).

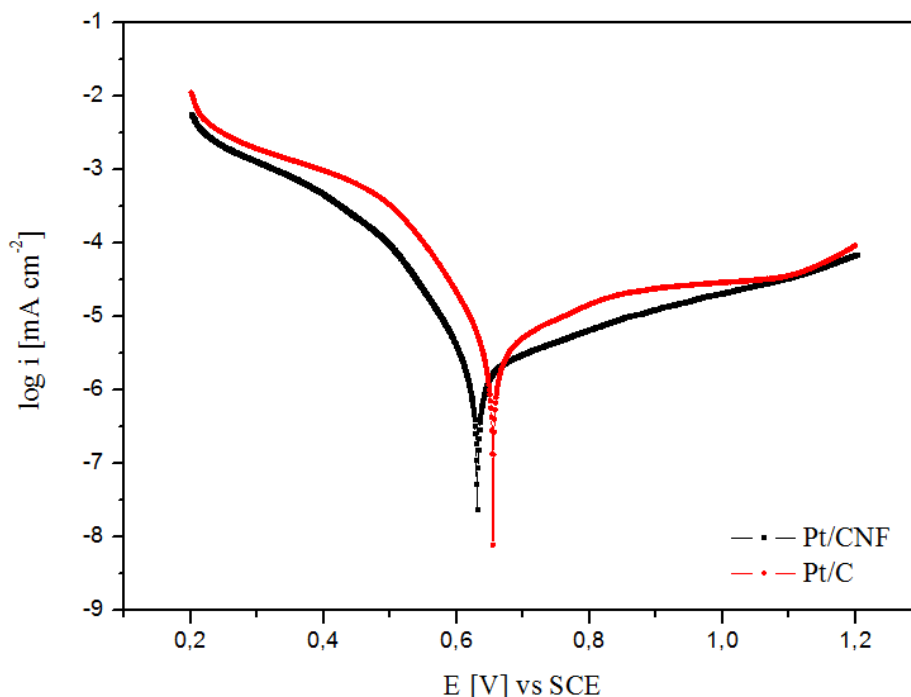


Figure 6. Potentiodynamic polarization curves for Pt/C and Pt/CNF based electrodes in 0.5 M H₂SO₄ aqueous solution, scan rate 0.16 mV s⁻¹.

Corrosion rate for Pt/C based electrode material determined from Tafel extrapolation is significantly higher than the value measured for the experimental Pt/CNF catalyst. Results are presented in the , fact which is well correlated with other literature reports [35]. Moreover, it has been shown that the corrosion resistance is strongly related to the graphitic character of the carbon structures [36]. Consequently, the higher graphitization degree of the CNF samples leads to a higher corrosion resistance of the material in comparison to carbon black based electrodes.

Table 5. For the investigated specimens, CNF based electrode is more stable in acid environment in comparison to carbon black electrode, fact which is well correlated with other literature reports [35]. Moreover, it has been shown that the corrosion resistance is strongly related to the graphitic character of the carbon structures [36]. Consequently, the higher graphitization degree of the CNF samples leads to a higher corrosion resistance of the material in comparison to carbon black based electrodes.

Table 5. Corrosion current and corrosion potential of investigated PEMFC electrode samples from Tafel extrapolation

	Pt/CNF	Pt/C
i_{corr} [$\mu\text{A cm}^{-2}$]	$1.87 \cdot 10^{-6}$	$3.71 \cdot 10^{-6}$
E_{corr} [V vs. SCE]	0.63	0.65
β_a [mV dec ⁻¹]	305	248
β_c [mV dec ⁻¹]	-74.5	-72.8
Corr [$\mu\text{m year}^{-1}$]	21.88	44.19

MEA testing is performed at ambient conditions (room temperature) with atmospheric air and pure hydrogen without additional humidification. Hydrogen is circulated through the anode with 0.2 bar overpressure with high excess gas in order to prevent hydrogen starvation over the active cell area. Air is pumped through the cathode. The cathode outlet is open to atmosphere. Stoichiometry factor is controlled to $\lambda = 4$. Polarization curve of a MEA with Pt/CNF based anode prepared according to the determined optimized pre-treatment parameters (120 W for 10 min) is shown in Fig 7. Furthermore, a MEA with typical Pt/C catalyst based anode is analyzed. Values for OCV and polarization behavior have been determined after MEAs are conditioned by a fast cycling procedure in constant voltage mode. Cell voltage is hold for 15 seconds at 0.65 V, 0.40 V and 0.15 V, consecutively. This procedure is repeated 50 times.

OCV for the Pt/CNF based sample is 0.95 V and 0.94 V for Pt/C based sample, respectively. For the optimized Pt/CNF based MEA maximum power density of 0.25 W cm^{-2} is obtained at a cell voltage of 0.45 V. This is 37% higher than for the Pt/C based MEA (0.18 W cm^{-2} at 0.40 V). As it was already described, a higher graphitization degree has been found for Pt/CNF based samples. This leads to higher electrical conductivity of the CL. As a result, ohmic voltage drop due to electrical resistance is decreased in comparison to Pt/C based electrodes.

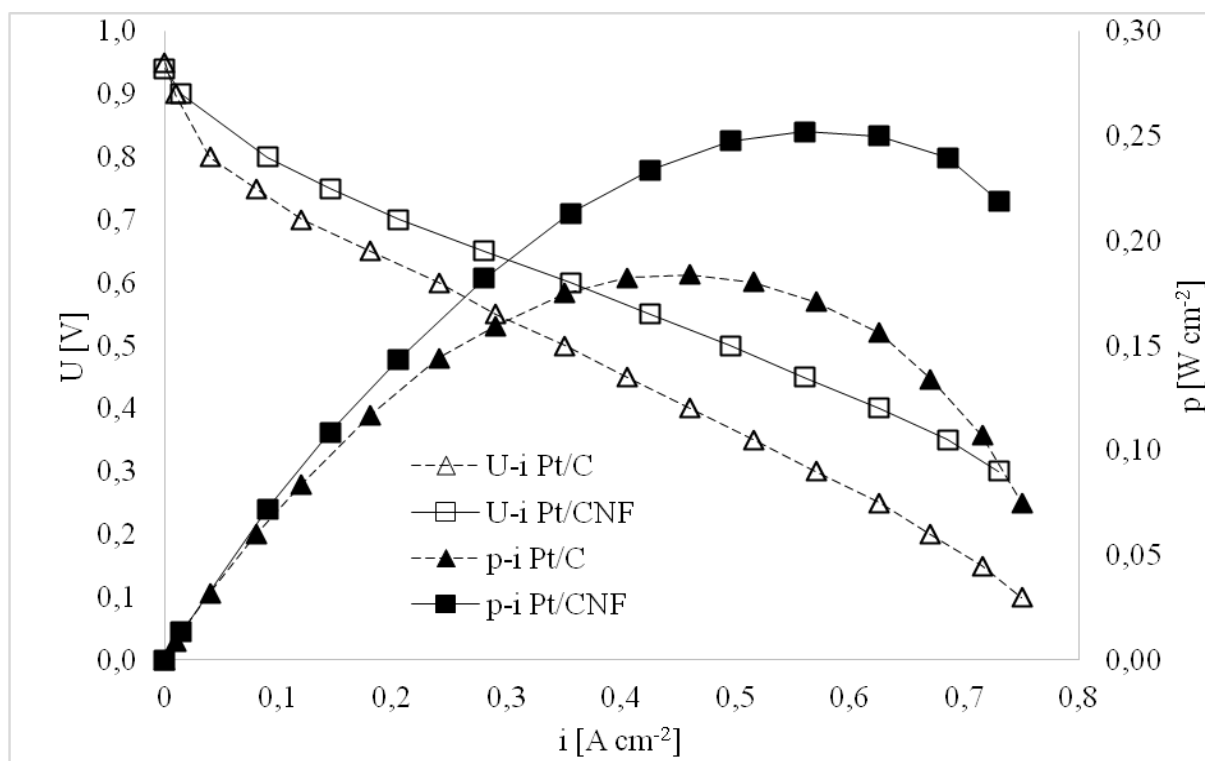


Figure 7. In-situ polarization behavior of Pt/C and Pt/CNF based MEA samples.

Furthermore, according to

Table 3 platinum loading for the Pt/C based anode is about 25% higher than for the Pt/CNF sample. The significant difference in specific power output as well as in platinum utilization may result from a high number of electrochemical active particles within the Pt/CNF based CL due to the optimized electrode preparation.

4. CONCLUSIONS

The high graphitization degree of about 90% for CNFs investigated in this study, is favorably for PEMFC electrodes. In terms of electrical conductivity and corrosion stability of the CNF based electrodes show better performance than typically Pt/C based electrodes.

An optimized preparation method for PEMFC anodes based on spray coated CNFs with subsequent platinum deposition has been presented in this experimental work. From the SEM micrographs fractured sample it can be concluded that particles are mainly located on top of the CNF layer, which leads to higher Pt utilization than for typical Pt/C based electrodes.

The oxygen plasma treatment performed previously to catalyst deposition affects platinum loading, ECSA and consequently the power density of prepared MEAs for PEMFCs by formation of functional groups at the fibers surface. Higher plasma power leads to increased etching phenomena which interrupts graphene layers of the treated fibers and decreases formation of functional groups. Therefore, an activation process with plasma power below 150 W is suggested. An optimized pre-treatment procedure in radio frequency induced oxygen plasma is achieved using 120 W plasma power and an exposure time of 10 minutes.

ACKNOWLEDGEMENTS

The presented results are carried out in a research project funded by the Ministry of Innovation, Science and Research of North Rhine Westphalia, Germany within the scope of the Ziel2.NRW program "Regionale Wettbewerbsfähigkeit und Beschäftigung – EFRE" (funding number: 005-1111-0010). Furthermore, we gratefully acknowledge the support by Grupo Antolin for providing the investigated CNFs. We also thank Mrs. Monica Meuris from Technical University of Dortmund for providing SEM as well as TEM images.

References

1. D. Stolten, Hydrogen and Fuel Cells, Wiley-VCH, (2010) Weinheim, Germany.
2. F. Barbir, Proton Exchange Membrane Fuel Cells - Theory and Practice, Second Edition, Academic Press, (2013) Waltham - USA.
3. Z. JiuJun, PEM Fuel Cell Electrocatalysts and Catalyst Layers - Fundamentals and Applications, Springer, (2008) London – UK, Chapter 1: pp. 1-88.
4. T. R. Ralph and M. P. Hogarth, *Platinum Metals Review*, 46 (2002) 3.
5. A. Therdthianwong, P. Saenwiset and S. Therdthianwong, *Fuel*, 91 (2012) 192.
6. G. Sasikumara, J. W. Ihma and H. Ryu, *Electrochim. Acta*, 50 (2004) 601.
7. S. Litster and G. McLean, *J. Power Sources*, 130 (2004) 61.
8. C. Sung, C. Liua and C. C. J. Cheng, *Int. J. Hydrogen Energy*, 39 (2014) 11700.
9. A. A. Fedotov, S. A. Grigoriev, P. Millet and V. N. Fateev, *Int. J. Hydrogen Energy*, 38 (2013) 8568.

10. A. Bonnefont, P. Ruvinsky, M. Rouhet, A. Orfanidi, S. Neophytides and E. Savinova, *WIREs Energy Environ.*, 3 (2014) 505.
11. L. Calvillo, M. Gangeri, S. Perathoner, G. Centi, R. Moliner and M. J. Lazaro, *Int. J. Hydrogen Energy*, 36 (2011) 9805.
12. F. J. Nores-Pondal, I. M. J. Vilella, H. Troiani, M. Granada, S. R. Miguel, O. A. Scelza and H. R. Corti, *Int. J. Hydrogen Energy*, 34 (2009) 8193.
13. Y. Shao, J. Wang, R. Kou, M. Engelhard, J. Liu, Y. Wang and Y. Lin, *Electrochim. Acta*, 54 (2009) 3109.
14. A. N. Golikand, M. Asgari and E. Lohrasbi, *Int. J. Hydrogen Energy*, 36 (2011) 13317.
15. X. Zhang, Y. Ye, Wang H and Yao S. Radiat, *Phys. Chem.*, 79 (2010) 1058.
16. Y. Chen, G. Zhang, J. Ma, Y. Zhou, Y. Tang and T. Lu, *Int. J. Hydrogen Energy*, 35 (2010) 10109.
17. M. J. Larsen and E. M. Skou, *J. Power Sources*, 202 (2012) 35.
18. A. Marinkas, F. Arena, J. Mitzel, G. M. Prinz, A. Heinzl, V. Peinecke and H. Natter, *Carbon*, 58 (2013) 139.
19. H. Wu, D. Wexler and H. Liu, *J. Solid State Electrochem.*, 15 (2011) 1057.
20. P. Morgan, *Carbon Fibers and their Composites*, Taylor & Francis, (2005) Boca Raton, USA.
21. W. Brandl and G. Marginean, *Thin Solid Films*, 447-448 (2004) 181.
22. V. Chirila, G. Marginean and W. Brandl, *Surf. Coat. Technol.*, 200 (2005) 548.
23. H. Bubert, W. Brandl, S. Kittel, G. Marginean and D. Toma, *Anal. Bioanal. Chem.*, 374 (2002) 1237.
24. G. Moral, EU patent 1 990 449 B1 (2012).
25. W. Weisenberger, I. Martin-Gullon, J. Vera-Agullo, H. Varela-Rizo, C. Merino, R. Andrews, D. Qian and Terry Rantell, *Carbon*, 47 (2009) 2211.
26. S. Woo, I. Kim, J. K. Lee, S. Bong, J. Lee and H. Kim, *Electrochim. Acta*, 56 (2011) 3036.
27. U. Rost, R. Muntean, P. Podleschny, G. Marginean, M. Brodmann, V. A. Şerban, *Solid State Phenomena*, 254 (2016) 27.
28. S. Lertviriyapaisan and N. Tantavichet, *Int. J. Hydrogen Energy*, 35 (2010) 10464.
29. G. Marginean, *Vapour Grown Carbon Fibres*, Ruhr Universität Bochum, PhD thesis, 2004.
30. U. Rost and M. Brodmann, *Neuartige Messvorrichtung basierend auf hydraulischer Verpressung zur Untersuchung von Brennstoffzellen und Elektrolyseurkomponenten*, IEEE Workshop Industrielle Messtechnik & Kraftfahrzeugsensorik, Instrumentation and Measurement Section, Mülheim – Germany, 2014, 11.
31. U. Rost, C. Mutascu, J. Roth, C. Sagewka and M. Brodmann, *J. Energy Power Eng.*, 9 (2015) 775.
32. M. M. Baizer, *Organic Electrochemistry*, Marcel Dekker, 1973 New York, USA
33. Z. JiuJun, *PEM Fuel Cell Electrocatalysts and Catalyst Layers - Fundamentals and Applications*, Springer, (2008) London – UK, Chapter 3: pp. 135-164.
34. R. Chetty, K. K. Maniam, W. Schuhmann and M. Muhler, *ChemPlusChem*, 80 (2015) 130.
35. F. N. Büchi, M. Inaba, T. J. Schmidt, *Polymer Electrolyte Fuel Cell Durability*, Springer, (2009) New York – USA, Chapter 2: pp. 7-56.
36. H.-S. Oh, K. H. Lim, B. Roh, I. Hwang, H. Kim, *Electrochim. Acta*, 54 (2009) 6515